SYMMETRY-RESTORING CRISES, PERIOD-ADDING AND CHAOTIC TRANSITIONS IN THE CUBIC VAN DER POL OSCILLATOR

Miguel A. F. Sanjuán

*Departamento de Física e Instalaciones, E.T.S. de Arquitectura,
Universidad Politécnica de Madrid, 28040 Madrid, Spain*

A generalization of the van der Pol oscillator, in which a cubic non-linearity in the restoring force is considered, has been studied. For very small values of the cubic parameter, different chaotic transitions take place, via period-doubling, saddle-node bifurcations and crises, which restore the symmetry of the chaotic attractor. For larger values of the parameter a period-adding sequence of saddle-node bifurcations and the scaling laws that rule them are found. When negative values of the cubic parameter are considered, bifurcations via hysteresis following a period-adding sequence are found. Finally, it has been found that there is a strong sensitivity to very small modifications of some system parameters.

© 1996 Academic Press Limited

1. INTRODUCTION

The possibility of irregular and aperiodic oscillations has manifested itself as one of the most interesting and striking properties of driven non-linear oscillators. A certain dynamical system may evolve toward this aperiodic dynamical state through different ways, showing that there are many different scenarios for the transitions to chaos [1], which are possible for dynamical systems when an appropriate parameter is varied.

Non-linear oscillators may be divided into two different types: self-excited oscillators, which possess a stable limit cycle without external driving, and strictly dissipative oscillators which tend to a motionless state when not driven.

The present work is concerned with a generalized version of a self-excited oscillator, the well-known van der Pol oscillator, in which a cubic term in the restoring force is considered. The equation of motion of the forced oscillator is

$$\mathrm{d}^2x/\mathrm{d}t^2 - a(1 - x^2)\,\mathrm{d}x/\mathrm{d}t + bx + cx^3 = d\sin\omega t, \tag{1}$$

where a, b, c, d and ω are parameters. This non-linear oscillator involves the non-linear damping term, corresponding to the classical van der Pol equation, and the non-linear cubic term, corresponding to the Duffing equation. Sometimes it is referred to as the Duffing–van der Pol oscillator.

In this study of the cubic van der Pol oscillator, a set of parameters has been selected for which the system is in a chaotic state, $a = d = 5$, $b = 1$, $c = 0$ and $\omega = 2\cdot466$ [2, 3].

The effect of the cubic term on the asymptotic behaviour of the system dynamics is the matter of interest, with c acting as the control and bifurcation parameter. The dynamics of equation (1) have been simulated by using a fixed-step-size fourth order Runge–Kutta numerical integration, with 500 time steps per forcing period. The oscillator is symmetric,

and thus the attractors appear either in pairs, being inversions of each other, or alone, being inversion-symmetric with an odd period [4]. The co-existence of asymmetric attractors is a feature of the van der Pol oscillator, due to its symmetry. The orbit loses stability and two stable asymmetrical orbits appear via a symmetry-breaking bifurcation, which corresponds in fact to the first period-doubling bifurcation. For very small values of c, different bifurcation phenomena are observed in this region, including saddle-node, period-doubling, period-adding and, due to the symmetry of the system, symmetry-breaking bifurcations, along with periodic and chaotic attractors. Note that without these symmetry-breaking bifurcations period-doubling bifurcations are not possible.

In the region [0, 0·02] five different chaotic zones have been found, instead of the three reported in reference [2], and an interpretation is to be given here of what was also reported there concerning symmetrical and unsymmetrical transitions to chaos. In Figure 1, the bifurcation diagram versus the parameter c of the cubic term for the parameter region [0, 0·015] is shown, where the five chaotic zones are clearly observed. A deeper study of this region shows a richer variety of complex dynamical phenomena, which occur in this system for very small values of the cubic non-linearity.

Among the different complex phenomena observed in the study of the dynamics of different non-linear oscillators, much attention has been focused on period-doubling bifurcations. However, other kinds of period-increasing phenomena, such as period-adding bifurcations, have received some attention very recently [5–9] and are therefore of interest. For larger values of the parameter c, a sequence of period-adding bifurcations leads the system to a period-1 orbit. Something similar occurs for negative values of c, where bifurcations via hysteresis are found. The system also shows a very strong sensitivity to very small modifications of some parameters, allowing transitions from chaotic to periodic states and *vice versa*.
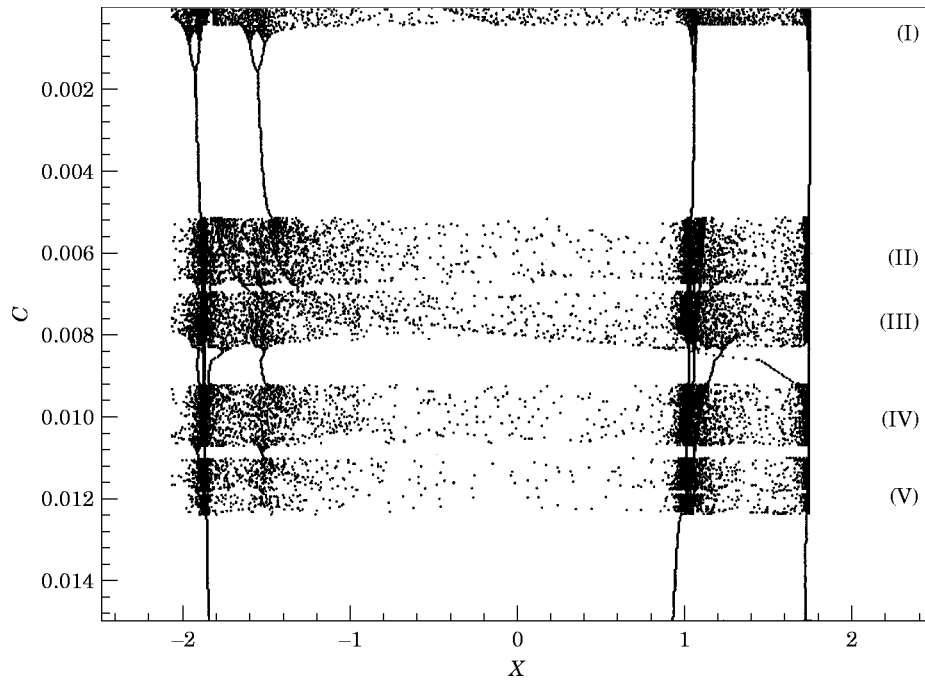

Figure 1. Bifurcation diagram versus the parameter c of the cubic term. The five chaotic regions in the c interval [0, 0·0015] are clearly observed. Other smaller windows exist within these regions.

2. CHAOTIC TRANSITIONS AND CRISES

As c increases different bifurcation phenomena and other features are observed. In Figure 2(a) the bifurcation diagram versus the cubic parameter for this region I, which is the same as region I in reference [2], is shown. At $c = 0.02$ one has a periodic orbit, which lies in a periodic window, extending until $c = 0.052$.

If one considers c as a decreasing parameter, a period-doubling bifurcation occurs at $c \approx 0.0015$. The symmetric chaotic attractor persists until $c = 0.0003$, where different attractors merge. At $c = 0.00044$ a sudden widening of the attractor occurs. In fact this is an interior crisis [10]. Figure 2(b) shows the asymmetric chaotic attractor at $c = 0.00045$, while Figure 2(c) shows the restored symmetric chaotic attractor at $c = 0.00043$, once the parameter has surpassed the value of the crisis. Figure 2(d) manifests a more symmetric chaotic attractor at $c = 0.00025$, taking further the limit value where the attractor merging crisis [11] at $c = 0.0003$ occurs. This crisis occurs in systems with symmetries where two or more chaotic attractors merge to form one chaotic attractor. The asymmetric chaotic attractor at $c = 0.00045$, which is shown in Figure 2(b), is explained by considering the unsymmetric chaotic bands before the interior crisis where the orbit lies. This may be observed very clearly in Figure 2(a). The chaotic attractor lies, in reality, in a four-chaotic
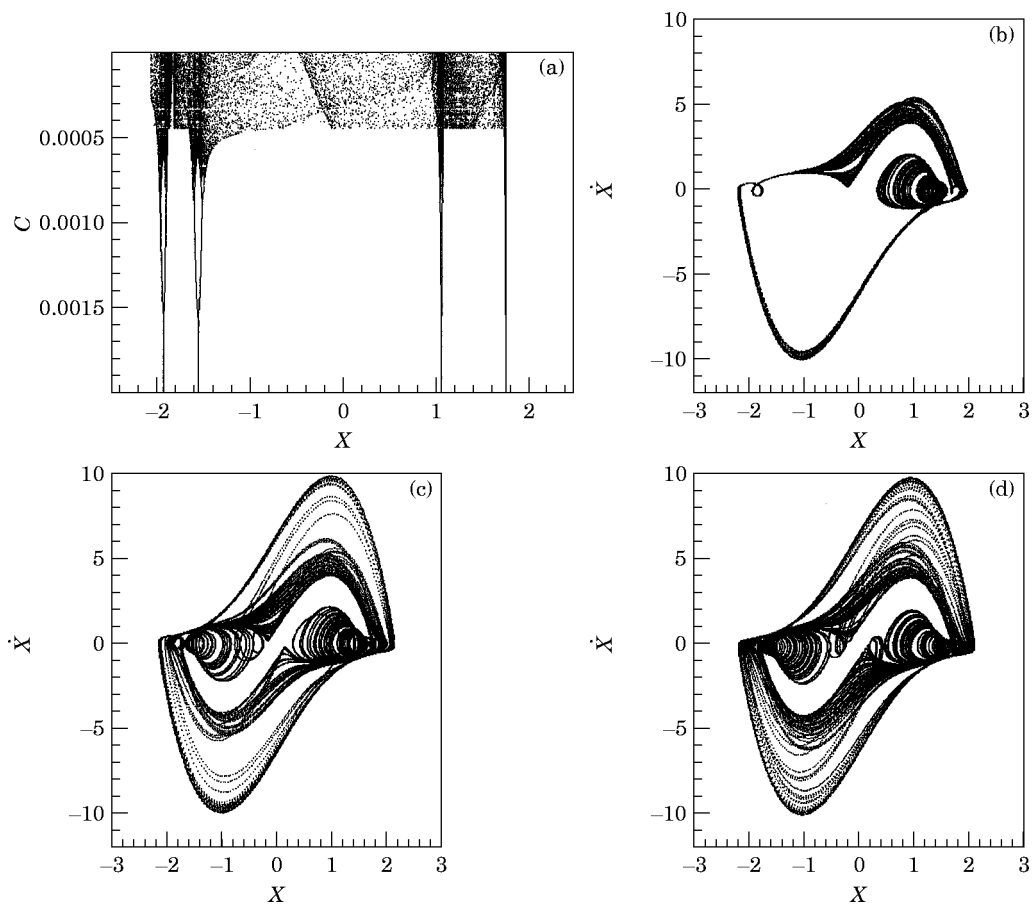

Figure 2. (a) Bifurcation diagram of region I; (b) asymmetrical chaotic attractor for $c = 0.00045$; (c) chaotic attractor for $c = 0.00043$ after the interior crisis, where the symmetry has been restored; (d) chaotic attractor for $c = 0.00025$.
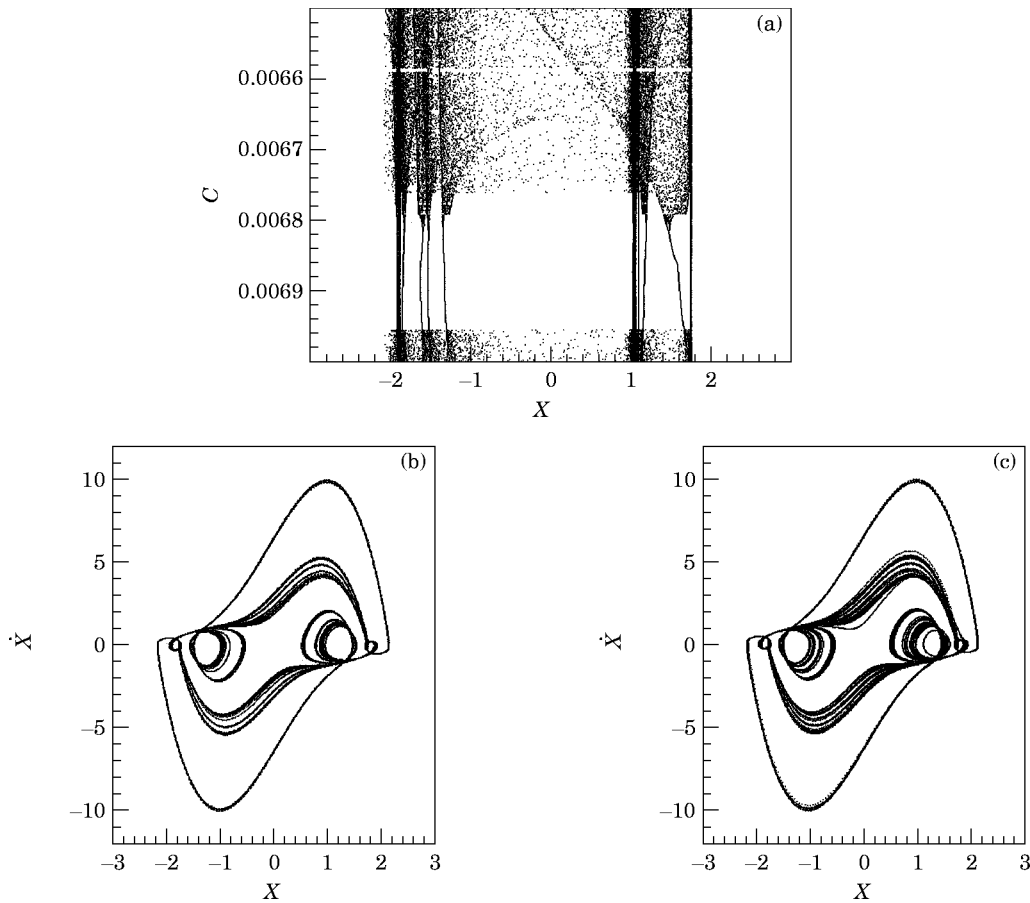
Figure 3. (a) Bifurcation diagram of region II; (b) chaotic attractor for $c = 0.00678$, where the orbit lies in a chaotic band attractor; (c) chaotic attractor for $c = 0.00675$, after the crisis.

band just before the interior crisis, which has the effect of widening the attractor into one chaotic band and consequently restoring the symmetry. This explains one of the routes described in reference [2]. In fact the route to chaos followed here is simply a period-doubling bifurcation route, which for certain parameter values allows the orbit to lie in an attractor formed by unsymmetric four-chaotic bands, just before the interior crisis where the symmetry is restored again.

The region II (see Figure 3(a)) extends approximately until $c = 0.00695$. When one considers the transition from a periodic orbit to the chaotic zone for decreasing values of c, one finds that at $c = 0.00686$ a symmetry-breaking bifurcation occurs. Figures 3(b) and 3(c) show the chaotic attractors in phase space before and after the interior crisis which exists at $c = 0.00676$, where the attractor widens notably. In this region the chaotic attractor lies within several chaotic bands, possessing a certain degree of symmetry for $c = 0.00678$, which is shown in Figure 3(b). Inside the chaotic region and past the crisis, a small periodic window at $c = 0.00659$ is found.

The region III, which extends until $c = 0.092$, is shown in Figure 4(a). Considering decreasing values of c as well, one observes at $c = 0.00864$ a symmetry-breaking bifurcation. Again the scenario leading to chaos is via period-doubling cascades. At $c = 0.00835$ the orbit lies within chaotic bands and, as the parameter decreases, the
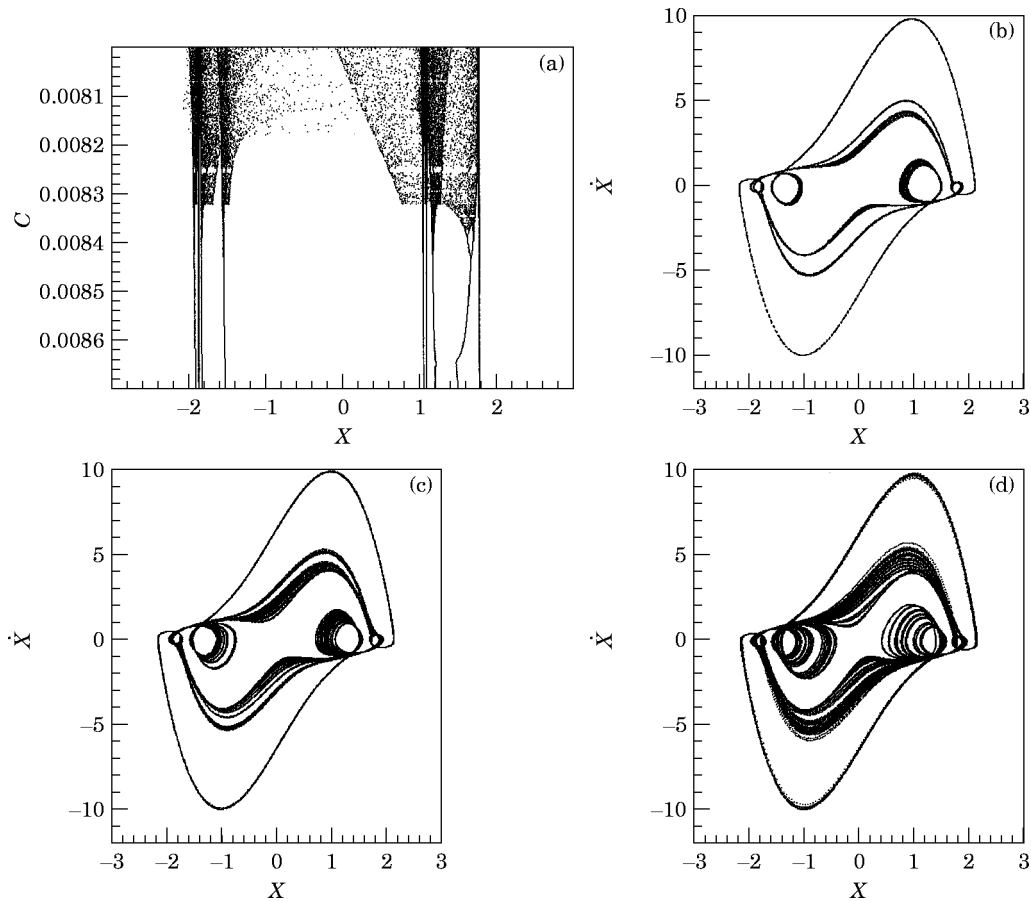
Figure 4. (a) Bifurcation diagram of region III; (b) chaotic band attractor for $c = 0.00835$; (c) chaotic attractor for $c = 0.0083$; (d) chaotic attractor for $c = 0.00818$.

symmetry increases. Figures 4(b) and 4(c) show the transition to wider chaotic bands with symmetry, while in Figure 4(d) one can see the more symmetric attractor for $c = 0.00818$, where the interior crisis takes place. Periodic windows beyond this parameter value are also observed.

Figure 5(a) shows the region IV, which corresponds to region II in reference [2], and continues until $c = 0.01102$. At $c = 0.011$ the oscillator has an asymmetric period-6 orbit as is shown in Figure 5(b). At $c = 0.01075$, just before the sudden widening of the chaotic attractor as shown in Figure 5(c), there is an asymmetrical chaotic attractor. This was not observed in reference [2], where it was stated that a chaotic unsymmetric attractor between a periodic unsymmetric and chaotic symmetric attractor was not found. The chaotic transition here is then similar to the one in region I. The period-doubling bifurcation cascades, at this value of the parameter, have chaotic bands which are non-symmetric until they reach the interior crisis at $c = 0.0107$, beyond the interior crisis and where the symmetry is restored again. This asymmetry at $c = 0.01075$ can be also observed in the time series for the velocity, which is shown in Figure 6.

Region V is the last chaotic zone in Figure 1, which corresponds to region III in reference [2]. It begins with a saddle-node bifurcation at $c = 0.1102$ from a period-6 orbit and ends up with a saddle-node bifurcation at $c = 0.0122$, where a period-3 orbit is born. Thus,
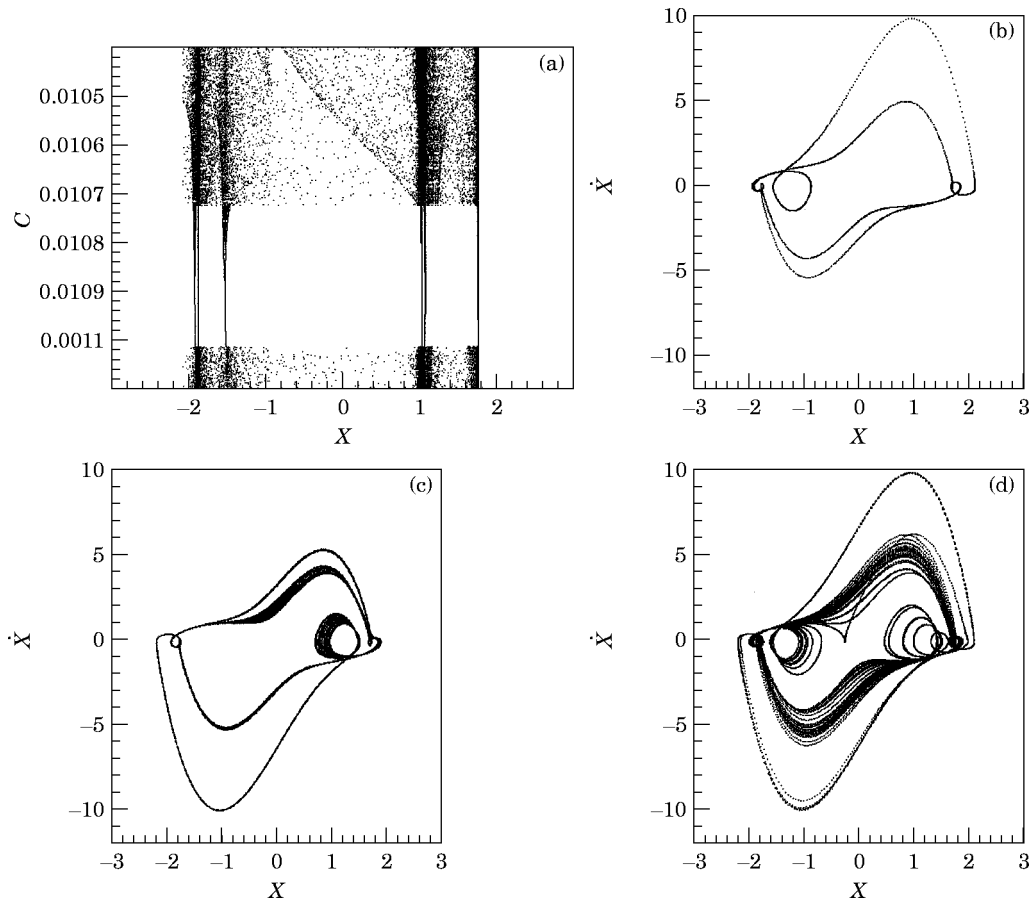
Figure 5. (a) Bifurcation diagram of region IV; (b) periodic attractor for $c = 0.011$; (c) asymmetric chaotic attractor for $c = 0.01075$; (d) chaotic attractor for $c = 0.0107$, after the interior crisis.

if one starts at a value of $c > 0.0122$, and decreases c, the periodic attractor suddenly undergoes a jump transition to the symmetric chaotic attractor at this point. Within the region, a small window of high periodicity may be observed between $c = 0.0118$ and $c = 0.0119$.

It should be noted here that similar sudden transitions from chaotic attractors into periodic attractors occur in any of the chaotic regions considered, at the value of the saddle-node bifurcation; that is, at $c = 0.0052$, $c = 0.00695$, $c = 0.092$ and $c = 0.01102$. Between two of these chaotic regions there is a periodic window, whose structure is universal in the sense that it is born through a saddle-node bifurcation, undergoes a period-doubling bifurcation and ends when the m-chaotic bands collide with the unstable periodic orbits. These were born at the same saddle-node bifurcation, where the chaotic bands widen into one band attractor at the interior crisis parameter value.

Thus five chaotic regions have been found in this c interval. In all of them the transitions to chaos are carried out through period-doubling bifurcation cascades, arriving then to a symmetric chaotic attractor, with the exception of this last region entered via decreasing values of c. In this final region a chaotic zone is entered through a saddle-node bifurcation giving rise to a symmetric attractor as well. The asymmetric chaotic attractors reported
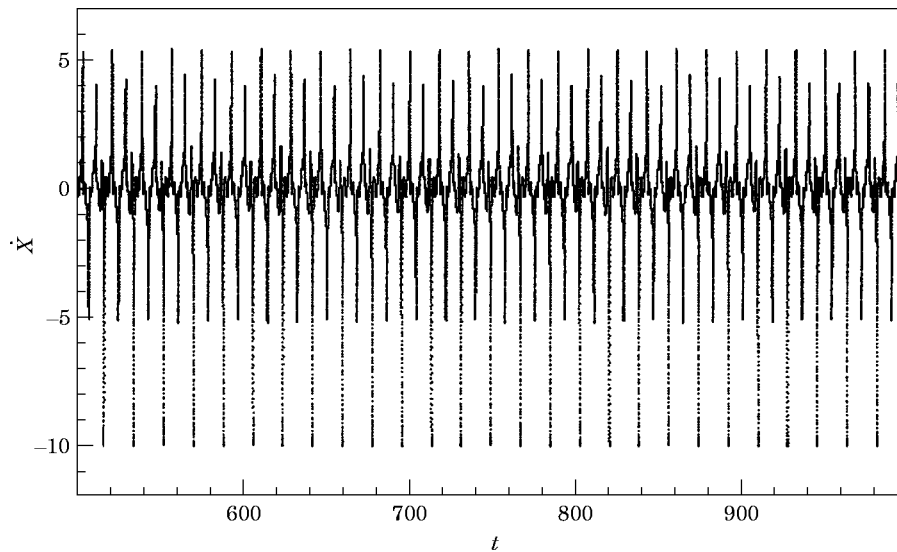
Figure 6. Time series for the velocity for $c = 0 \cdot 01075$, where the asymmetry is manifested.

in reference [2] are just the chaotic attractors corresponding to the chaotic bands before the interior crisis occurs. This restores the symmetry once the value of the crisis is exceeded.

3. PERIOD-ADDING AND SCALING LAWS

The period-3 window which appears at $c = 0 \cdot 0122$ in Figure 1 continues until $c = 0 \cdot 58$ where another saddle-node bifurcation occurs. Arising from this bifurcation, a series of periodic windows of increasing periodicity lead finally to a period-1 orbit at a saddle-node bifurcation when the parameter value is $c = 1 \cdot 659$, as illustrated in Figure 7.

In this parameter region an infinite cascade of saddle-node bifurcations is observed and a sequence of periodic windows of periods $3 \to 2 \to 5 \to 3 \to 7 \to 4 \to 9 \to \cdots$ is exhibited. This infinite sequence of saddle-node bifurcations accumulates at the value of $c = 1.659$, where the period-1 orbit is born via a saddle-node bifurcation. This infinite cascade of saddle-node bifurcations is composed of two subsequences of periodic windows, each one possessing a period-adding bifurcation mechanism. The first one arithmetically increases the period by 2 and the other one increases the period by 1. In fact what one really has is a period-1 adding sequence, since one of the subsequences corresponds to symmetric orbits, where the periodicity increases by two. The other subsequence corresponds to pairs of asymmetric orbits. However, only one of the asymmetric orbits is observed in the bifurcation diagram. Similar situations occur for the Duffing oscillator and for the linear van der Pol oscillator [12, 13]. On the other hand, the topological explanation of the window ordering and of the window-structure is given in reference [13], where the bifurcation structure of the double-well Duffing oscillator is analyzed in detail. As c increases, the size of the windows decreases, and the period m of the windows increases, accumulating at the final saddle-node bifurcation.

What one observes is that the length in c of the range of stability for an orbit of period m decreases approximately geometrically with m. One can analyze the scaling law and structure of this period-adding sequence as follows. Suppose $\{c_m\}_{m=3}^{\infty}$ is the series formed by the parameter values for which the cascade of saddle-node bifurcations occurs.
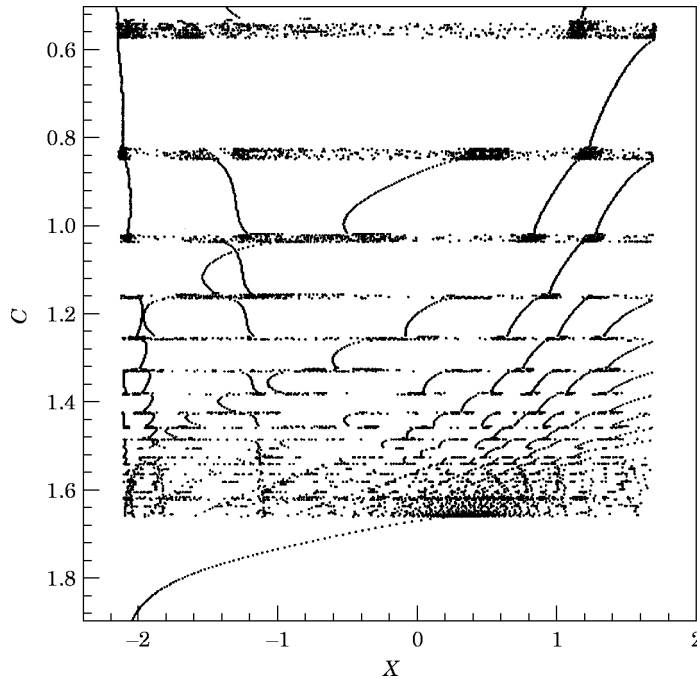
Figure 7. Sequence of period-adding bifurcations accumulating at $c = 1.659$, where a period-1 orbit is born via a saddle-node bifurcation.

One can construct a sequence of δ_m values,

$$\delta_m = (c_{m+2} - c_{m+1})/(c_{m+1} - c_m) = d_{m+1}/d_m, \tag{2}$$

where $d_m = c_{m+1} - c_m$ is the parameter length, between two successive bifurcations including the period-m window and the small chaotic band in between. For large values of c_m the period becomes larger and when $m \to \infty$, numerical calculations show that

$$\lim_{m \to \infty} \delta_m = \delta = 1. \tag{3}$$

This confirms the result given in reference [9], where δ is conjectured to be a universal constant for period-adding bifurcations. Likewise, the well-known Feigenbaum constant $\delta = 4.669$ applies to period-doubling bifurcations [1]. It is possible in this situation to predict the parameter value c_∞, to which the accumulation of these bifurcations values c_m tends as $m \to \infty$. This parameter value corresponds with the birth of the period-1 orbit through a saddle-node bifurcation, and obviously depends on the value of the parameter set (a, b, d, w) chosen. The Aitken δ^2-process [14] of quick convergence, which is applied to geometrically decreasing magnitudes, may be used in order to predict this parameter value. The result which is obtained is

$$c_\infty = c_m + d_m/(1 - \delta_m), \tag{4}$$

giving c_∞ with rather good accuracy. For instance, the period-34 orbit is born at a saddle-node bifurcation at $c_{34} = 1.6305$, which $c_{35} = 1.6322$ and $c_{36} = 1.6338$. Thus, $d_{34} = 0.0017$ and $\delta_{34} = 0.9411765$. These values predict an accumulation point at $c_\infty = 1.6594$. The scaling laws for c_m can also be analyzed. Figures 8(a, b) show the log-log plot of $c_\infty - c_m$ and $c_{m+1} - c_m$ versus the period m. It is clear that there is a power law relationship. For large values of m, the relationships obtained are $c_\infty - c_m \sim m^{-2}$ and
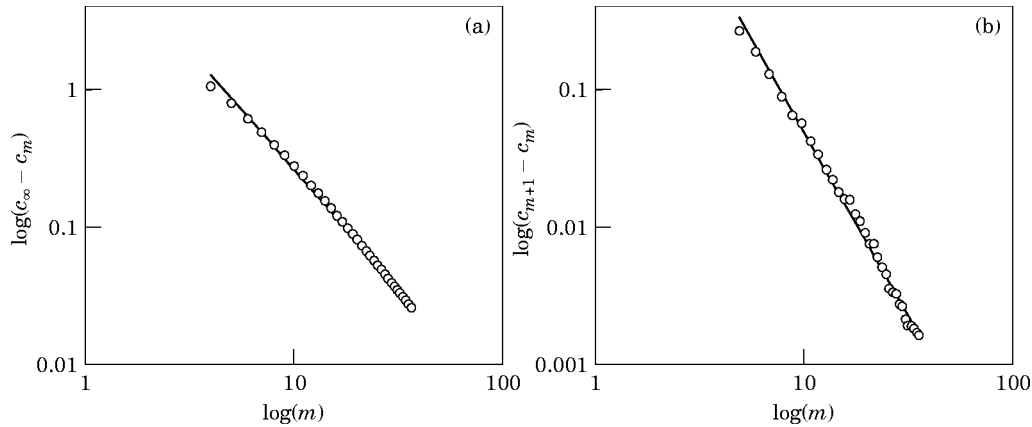
Figure 8. (a) Log-log plot of $c_\infty - c_m$ versus the period m – for large values of the period the scaling behaves as $c_\infty - c_m \sim m^{-2}$; (b) log-log plot of $c_{m+1} - c_m$ versus the period m– for large values of the period the scaling behaves as $c_{m+1} - c_m \sim m^{-3}$.

$c_{m+1} - c_m \sim m^{-3}$. Similar results were obtained in reference [15] for a one-dimensional mapping possessing a period-adding sequence. If one considers the relation (4), which holds especially for large values of m and the above scaling laws, one can conclude that $1 - \delta_m \sim m^{-1}$ for large values of m. This confirms the result of equation (3) and also gives the rate of convergence for large values of the period m.

4. BIFURCATION DIAGRAMS FOR NEGATIVE VALUES OF c

The bifurcation diagrams have also been obtained for negative values of c. In this case the potential from which the restoring force is derived is an inverted double-well, which corresponds to a soft spring oscillator. The topology of phase space changes from the previous case in such a way that the orbits are confined, when $b = 1$, to values of $|x| < \sqrt{1/c}$ within a separatrix or heteroclinic orbit. Here there is the possibility of escape when the energy of the system allows the orbit to overcome the potential barrier which for $b = 1$ is of the order of $1/(4c)$. What has been found is a rather small chaotic region for very small values of c in the interval $[-0·006, 0]$, where all the bifurcation phenomena reported for positive values of c, such as period-doubling, crisis and symmetry-breaking appear. After this small chaotic region (see Figure 9(a)), a period-5 orbit is born at $c = -0·006$ through a saddle-node bifurcation, and at $c \sim -0·15$ suddenly this system switches to a period-7 orbit, without traversing any chaotic region. In fact what one has here is a bifurcation via hysteresis, which may be observed when the parameter used for the bifurcation diagram is varied in the reversed direction. The region of the hysteresis extends from $c \sim -0·13$ to $c \sim -0·15$, where both period-7 and period-11 orbits co-exist. One enters into a chaotic region again, and finally the system suffers the sudden destruction of the period-11 attractor where the orbit lies, escaping from its potential well at the value of $c = -0·244$ and x tends to the attractor at $|x| = \infty$. For larger values of the forcing and the frequency, numerical calculations show the appearance of new periodicities (see Figure 9(b)). In fact the transition observed is chaos $\rightarrow 7 \rightarrow 9 \rightarrow 11 \rightarrow$ chaos $\rightarrow$ periodic window $\rightarrow$ chaos $\rightarrow$ boundary crisis [10], where the chaotic attractor collides with the periodic orbit of its basin boundary, and the system undergoes the escape from its potential to infinity, at a parameter value larger than before. The periods observed are odd and the period-adding involves adding by two to the previous
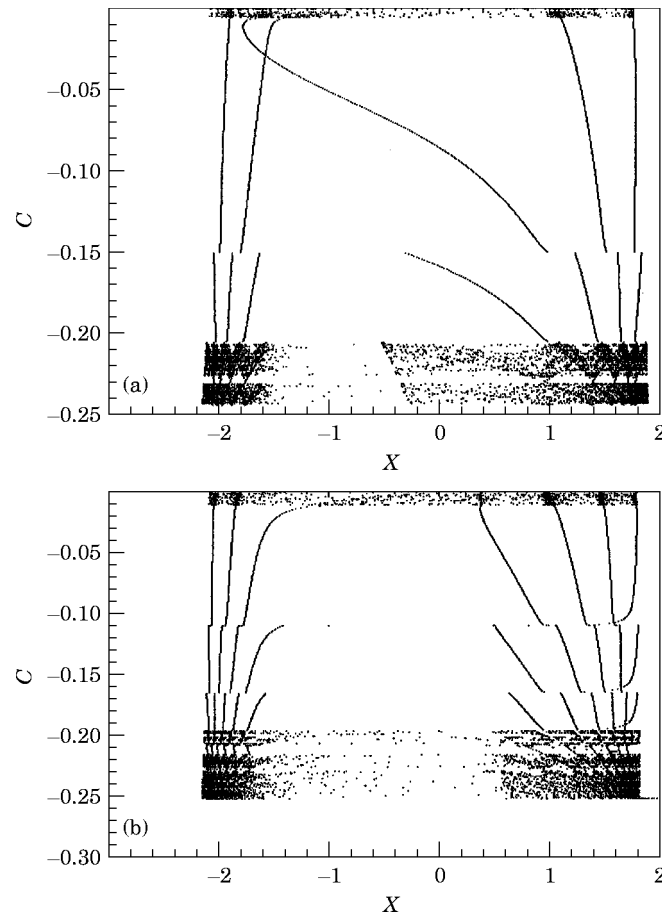
Figure 9. (a) Bifurcation diagram for negative values of the parameter c – at $c = -0.244$ the period-11 orbit collapses and escapes to an attractor at infinity; (b) bifurcation diagram for $d = 10$ and $\omega = 3.9$ versus negative values of c – boundary crisis is observed past $c = -0.25$.

period. For even larger values of the forcing and the frequency, the periodic-periodic transitions disappear, and what are observed are chaotic-periodic transitions. Also, the period-adding mechanism with odd periods adds two to the previous period. The scaling relations in the period-adding bifurcations, which are observed for the negative values of the parameter c, seem to possess the same laws as those described in the preceding section.

5. TRANSITIONS TO PERIODIC STATES

Another interesting phenomenon is the strong sensitivity to small changes in the parameters of the oscillator. Suppose one has a chaotic orbit for say $c = 0$. After a very small increase of c, say to $c = 0.003$, the situation also remains chaotic, in fact one is in the chaotic region before the crisis, as seen in Figure 1. Figure 10(a) indicates in phase space the effect of a small change in the damping term, now $a = 4.9861$, leading to an asymmetrical periodic state. It is interesting to note that for the same parameter of the damping term and making again $c = 0$, the orbit falls into a chaotic attractor, showing a very strong sensitivity to the modification of the parameters. For smaller values of the
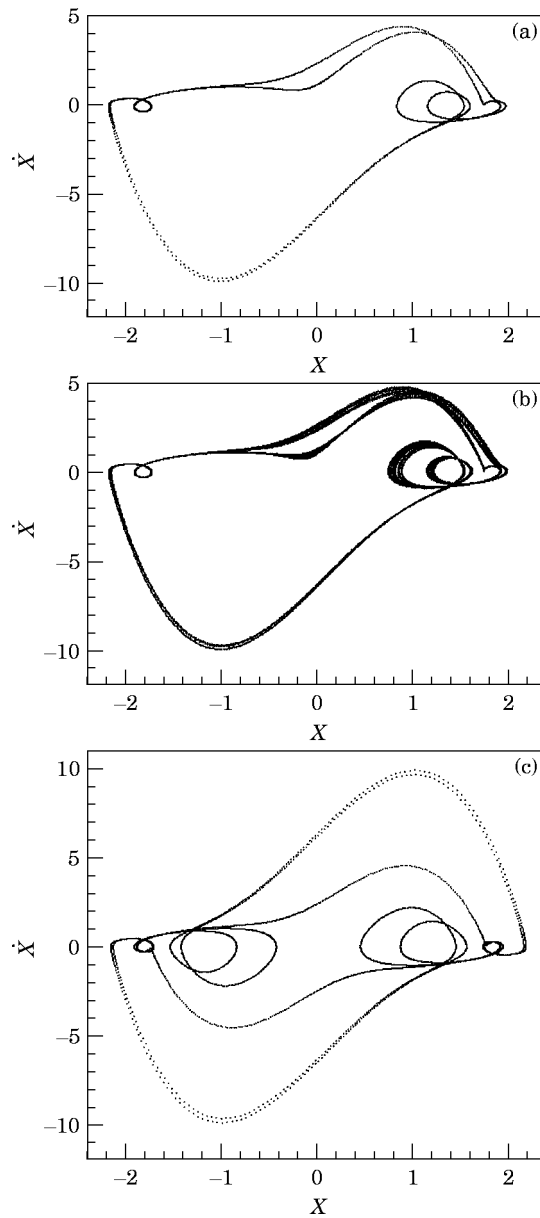
Figure 10. (a) Periodic attractor for $a = 4\cdot9861$ and $c = 0\cdot0003$; (b) chaotic attractor when c is reduced to zero. Observe the strong sensitivity to the transition from a chaotic state to a periodic state and *vice versa*; (c) periodic attractor for $b = 0\cdot995$ and $c = 0\cdot0003$. For $c = 0$ the attractor remains periodic.

damping parameter, the system becomes periodic with lower periodicity. Something similar may be observed by slightly varying the coefficient b of the linear term (see Figure 10(b)), although now this parameter is not as sensitive as before, since the orbit also remains periodic for $c = 0$.

One intuitive explanation of this phenomenon lies in the observation that there are many periodic windows inside the chaotic area, which can be observed in a certain bifurcation diagram for a chosen set of parameters. If one varies some of the parameters a little, the

attractor changes substantially and may easily fall into one of the periodic windows inside the chaotic attractor, leading the system to a periodic orbit.

6. CONCLUSIONS

In the present work, it has been shown that chaotic transitions exist for very small values of the c parameter of the cubic term of the hard spring restoring force. Bifurcation phenomena and complex behaviour have been found in this small region of parameters, such as period-doubling bifurcations, symmetry-restoring crises via interior crises and attractor-merging crises and also saddle-node bifurcations. Basically there are two routes to chaos: period-doubling and the intermittency associated with the saddle-node bifurcations. An explanation has been given of some previous numerical experiments, via other features observed in this study. For larger values of the parameter, a sequence of period-adding bifurcations has been found and the scaling properties have been analyzed. These confirm recent conjectures about the universal character of this phenomenon. Similarly negative values of c, which describes a soft spring restoring force, have been considered. Bifurcations via hysteresis are produced along with boundary crises, where the system is attracted to infinity. Finally it has been shown that there is strong sensitivity to very small changes in the values of certain parameters, causing transitions from chaotic to periodic attractors. This suggests that the system is especially sensitive to very small variations of the parameters corresponding to the damping term and to the cubic term. Thus, it would be of interest to consider a parametric perturbation of one of the above mentioned parameters, by means of which an easy control [16] of the chaotic orbits of the system would be expected.

ACKNOWLEDGMENTS

REFERENCES

1. E. OTT 1993 *Chaos in dynamical systems*. Cambridge University Press. (For a good introduction on chaotic transitions, see chapter 8).
2. T. KAPITANIAK and W.-H. STEEB 1990 *Journal of Sound and Vibration* **143,** 167–170 Transition to chaos in a generalized van der Pol equation.
3. U. PARLITZ and W. LAUTERBORN 1987 *Physical Review A* **36,** 1428–1434 Period-doubling cascades and devil's staircases of the driven van der Pol oscillator.
4. R. RÄTY, J. VON BOEHM and H. M. ISOMÄKI 1984 *Physics Letters A* **103,** 289–292 Absence of inversion-symmetric limit cycles of even periods and the chaotic motion of Duffing's oscillator.
5. A. B. NORDMARK 1991 *Journal of Sound and Vibration* **145,** 279–297 Non-periodic motion caused by grazing incidence in an impact oscillator.
6. H. E. NUSSE, E. OTT and J. A. YORKE 1994 *Physical Review* E **49,** 1073–1076 Border-collision bifurcations: An explanation for observed bifurcation phenomena.
7. W. CHIN, E. OTT, H. E. NUSSE and C. GREBOGI 1994 *Physical Review* E **50,** 4427–4444 Grazing bifurcations in impact oscillators.
8. Y.-F. HUANG, T.-C. YEN and J.-L. CHERN 1995 *Physics Letters* A **199,** 70–74 Observation of period-adding in an optogalvanic circuit.

9. Y. S. FAN and T. R. CHAY 1995 *Physical Review* E 51, 1012–1019 Crisis and topological entropy.
10. C. GREBOGI, E. OTT and J. A. YORKE 1982 *Physical Review Letters* **48,** 1597–1510 Chaotic attractors in crisis.
11. C. GREBOGI, E. OTT, F. ROMEIRAS and J. A. YORKE 1987 *Physical Review A* **36,** 5365–5380 Critical components for crisis-induced intermittency.
12. V. ENGLISH and W. LAUTERBORN 1991 *Physical Review A* **44,** 916–924 Regular window structure of a double-well Duffing oscillator.
13. R. GILMORE and J. W. L. MCCALLUM 1995 *Physical Review* E **51,** 935–956 Structure in the bifurcation diagram of the Duffing oscillator.
14. W. H. PRESS, S. A. TEUKOLSKY, W. T. VETTERLING and B. P. FLANNERY 1992 *Numerical Recipes in C*. Cambridge University Press.
15. K. KANEKO 1983 *Progress of Theoretical Physics* **69,** 403–414 Similarity structure and scaling property of the period adding phenomena.
16. T. SHINBROT, C. GREBOGI, E. OTT and J. A. YORKE 1993 *Nature* **363,** 411–417 Using small perturbations to control chaos.
17. H. E. NUSSE and J. A. YORKE 1994 *Dynamics: Numerical Explorations*. New York: Springer-Verlag.